

# A design of speed reducer with trapezoidal tooth profile for robot manipulator<sup>†</sup>

Won-Ki Nam and Se-Hoon Oh\*

*Department of Mechanical Engineering, Chung-Ang University, Seoul 156-756, Korea*

(Manuscript Received March 3, 2010; Revised September 14, 2010; Accepted November 11, 2010)

## Abstract

Robots are increasingly performing human work as manufacturing is automated. Accordingly, the use of precision speed reducers has become essential for achieving precise control of the robot arm position. Curved tooth profiles, such as cycloid or involute tooth profiles, are generally used in precision speed reducers. Speed reducers with cycloid tooth profiles, which enable high precision control, are widely used to manipulate robot systems. This study proposes a speed reducer that has a trapezoidal tooth profile with straight lines. In this work, we mechanically analyzed trapezoidal tooth profiles, and then measured performance was by various tests using a prototype manufactured specifically for this study.

*Keywords:* Robot manipulator; Trapezoidal tooth profile; Speed reducer; Trajectory

## 1. Introduction

Planocentric gears reducers and harmonic drivers are generally used among the many types of speed reducers currently available for robots. The cycloid reducer (RV reducer) is the most common type of planocentric gear reducer in use today. Cycloid drives have been popular reducers from the 1930s until the present time due to their compact, light-weight, high speed reduction compared to planetary gear trains, together with their high mechanical advantage in a single stage [1]. However, there is backlash in the cycloid drive due to variations in machining, which will reduce stability and inherent noise and vibration, particularly at high speeds [2].

Most robots used for automated manufacturing employ harmonic drivers for the upper two or three joints and cycloid reducers for the base joints. In full-size robots, cycloid reducers are used for all six joints [3, 4]. Harmonic and cycloid reducers can exhibit significant speed reduction rates even at only one stage and are able to transfer large torques even at small sizes because of their much tooth gearing rates; thus, they are predominantly used for robots that require a compact

structure, large load capacity, and high-precision control of position [5]. These reducers are becoming increasingly specialized for applications such as measurement of tooth profile manufacturing techniques and assembly skills. With increasing demand for high functions in areas such as semiconductor manufacturing and the space industry, continued development of cycloid and harmonic reducers can be expected from the viewpoint of satisfying user requirements.

In designing tooth profile considering user requirements, the geometry of conjugate surfaces is of major concern in designing the gears and generating the conjugate meshing elements, and the meshing of gears and the generations of conjugate surfaces have been previously studied [6-10].

In this study, we designed a speed reducer for robots by introducing a novel trapezoidal tooth profile concept, and we conducted a tooth profile design program and we manufactured a prototype and measured its performance.

## 2. Methodology

### 2.1 Structure of speed reducer

The proposed reducer essentially consists of an inner gear with inner teeth that function collectively as a housing, an external gear that conducts eccentric movements, and an output part that generates reduced rotations. Generally, a cycloid

<sup>†</sup> This paper was recommended for publication in revised form by Associate Editor Jeong Sam Han

\*Corresponding author. Tel.: +82 2 820 5314, Fax.: +82 2 817 3135  
E-mail address: wonki@wm.cau.ac.kr

© KSME & Springer 2011

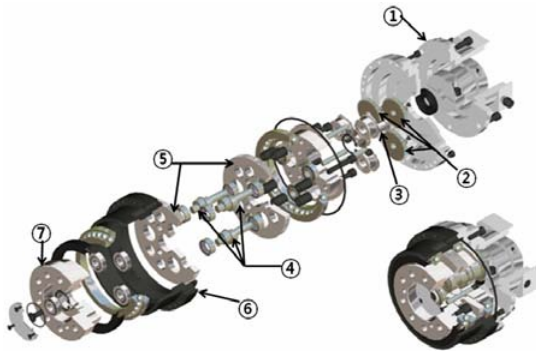


Fig. 1. Disassembly view of a robot reduction drive.

reducer can be categorized as a general cycloid reducer or one that contains a planetary gear. Fig. 1 shows the structure of a cycloid reducer that contains a planetary gear. Here, unlike in the general cycloid reducer, the input axis (③) from the motor generates power to rotate the planetary gear (②), and the eccentric axis (④) of the planetary gear moves the center position of the cycloid gear (⑤) at the moment when it makes tooth-by-tooth contact with the inner gear (⑥). This causes the cycloid gear turn on its own axis in a direction opposite to that of the input rotation, because the axis has an all-in-one structure. Cycloid reducers containing inner gears composed of pins or planetary gears, which exert a two-speed slowdown effect on the reducer system, have recently gained in popularity for robots. This is because they can yield a greater rate of speed reduction than general cycloid reducers of equal size, which reduce speed by translating cycloid gear motion directly through the input eccentric axis [11, 12].

**2.2 Definition of trapezoidal tooth profile**

General tooth profiles of gears have shapes corresponding to those of involute curves or cycloids. In this study, however, a trapezoidal tooth profile was used rather than the previously used involute or cycloid tooth profiles. The gearing features of a trapezoidal tooth profile have not yet been studied in depth because trapezoidal tooth profiles have hitherto been used mostly for cam devices that have cycloid movement. In our current study, we conducted an analysis to reveal the interference or gearing features of a trapezoidal tooth profile.

Assuming that the tooth number of an external gear is  $Z_1$ , that of a internal gear is  $Z_2$ , and the number of modules is  $m$ , the basic diameters of the external gear and internal gear are equal to  $D_1 = mZ_1$  and  $D_2 = mZ_2$ , respectively. The size of a tooth shown in Fig. 2 is equal to the value of the circumference length of a pitch circle divided by the number of teeth.

$$\left\{ \begin{array}{l} \frac{\pi D_1}{Z_1} = \frac{\pi m Z_1}{Z_1} = \pi m \\ \frac{\pi D_2}{Z_2} = \frac{\pi m Z_2}{Z_2} = \pi m \end{array} \right. \quad (1)$$

The tooth size is  $\pi m$ , as shown in Fig. 2. At this point, as-

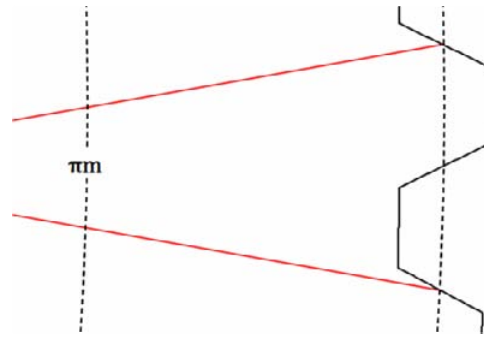


Fig. 2. Angular size of one tooth.

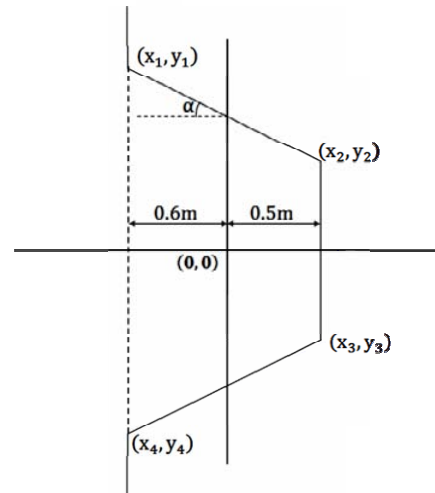


Fig. 3. Basic tooth profile for external gear.

suming that the ratio between the declination surface and the outer and inner surface of the tooth is constant, the size of the outer surface of the tooth is equal to  $m\pi / 4$ .

Assuming that the center of the tooth falls on the starting point at which the trapezoidal tooth profile of the external gear is defined, the following equations can be deduced.

$$\begin{cases} x_1 = -0.6 \times m \\ y_1 = \frac{\pi m}{4} - x_1 \times \tan \alpha \end{cases} \quad (2)$$

$$\begin{cases} x_2 = 0.5 \times m \\ y_2 = \frac{\pi m}{4} - x_2 \times \tan \alpha \end{cases} \quad (3)$$

$$\begin{cases} x_3 = x_2 \\ y_3 = -y_2 \end{cases} \quad (4)$$

$$\begin{cases} x_4 = x_1 \\ y_4 = -y_1 \end{cases} \quad (5)$$

In the same manner, the trapezoidal tooth profile can be defined as shown below; however, the amount of eccentric movement of the external gear must also be considered at the position where the tooth profile of the internal gear is defined.

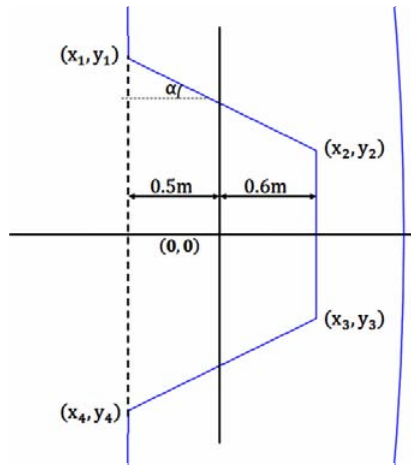


Fig. 4. Basic tooth profile for internal gear.

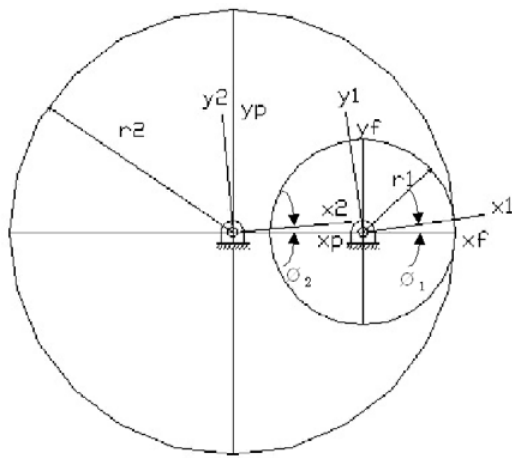


Fig. 5. Kinematic modeling of pin trajectory.

$$\begin{cases} x_1 = -0.5 \times m + (e-1) \times m \\ y_1 = \frac{\pi m}{4} - x_1 \times \tan \alpha - (e-1) \times m \end{cases} \quad (6)$$

$$\begin{cases} x_2 = 0.6 \times m + (e-1) \times m \\ y_2 = \frac{\pi m}{4} - x_2 \times \tan \alpha - (e-1) \times m \end{cases} \quad (7)$$

$$\begin{cases} x_3 = x_2 \\ y_3 = -y_2 \end{cases} \quad (8)$$

$$\begin{cases} x_4 = x_1 \\ y_4 = -y_1 \end{cases} \quad (9)$$

In these equations,  $e$  represents the amount of eccentric movement.

### 2.3 Tooth profile kinematics equation

In a cycloid reducer, the external tooth wheel exhibits eccentric cam movement. The amount of eccentric movement can be controlled as shown below, and the tooth profile movement can change according to predictable values. Fig. 5 shows the

results of kinematic pin trajectory modeling.

The pitch circles of the external gear and the internal gear can be defined as follows [13]:

$$r_1 = \frac{mZ_1}{2} \quad (10)$$

$$r_2 = \frac{mZ_2}{2} \quad (11)$$

where as in the tooth profile module,  $m$  is equal to the pitch circle diameter,  $D$ , divided by the number of teeth,  $Z$ , in units of millimeters.  $Z_1$  and  $Z_2$  indicate the number of teeth in the internal and the external gear, respectively.

If the larger pitch circle rotates, the two pitch circles must rotate in the same direction simultaneously, and it is like the two rotate at constant but different angular speeds.

$$r_1 \phi_1 = r_2 \phi_2 \quad (12)$$

where  $\phi_1$  and  $\phi_2$  denote the angular speed when the inner and the external tooth wheels rotate, respectively. Eq. (13) immediately below shows the variation in Eq. (12) for  $\phi_1$ .

$$\phi_1 = \frac{r_2}{r_1} \phi_2 = \frac{Z_2}{Z_1} \phi_2 \quad (13)$$

Meanwhile, Eq. (14) can be used to calculate the absolute angular speed when the external tooth wheel rotates and revolves with the inner tooth wheel fixed.

$$\phi_1 - \phi_2 = \left( \frac{Z_2}{Z_1} - 1 \right) \phi_2 = \left( \frac{Z_2 - Z_1}{Z_1} \right) \phi_2 \quad (14)$$

The position coordinates of the external tooth wheel can be calculated from those of the inner tooth wheel by using the following equations:

$$r_1 = M_{12} r_2 \quad (15)$$

$$M_{12} = M_{1f} M_{fp} M_{p2} \quad (16)$$

$$r_2 = [x_2 \quad y_2 \quad 0 \quad 1]^T \quad (17)$$

$$M_{1f} = \begin{bmatrix} \cos \phi_1 & \sin \phi_1 & 0 & 0 \\ -\sin \phi_1 & \cos \phi_1 & 0 & 0 \\ 0 & 0 & 1 & 0 \\ 0 & 0 & 0 & 1 \end{bmatrix} \quad (18)$$

$$M_{fp} = \begin{bmatrix} 1 & 0 & 0 & -e \\ 0 & 1 & 0 & 0 \\ 0 & 0 & 1 & 0 \\ 0 & 0 & 0 & 1 \end{bmatrix} \quad (19)$$

$$M_{p2} = \begin{bmatrix} \cos \phi_2 & -\sin \phi_2 & 0 & 0 \\ \sin \phi_2 & \cos \phi_2 & 0 & 0 \\ 0 & 0 & 1 & 0 \\ 0 & 0 & 0 & 1 \end{bmatrix} \quad (20)$$

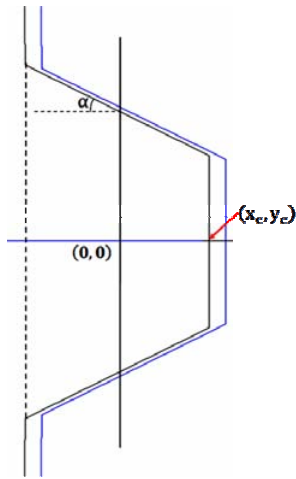


Fig. 6. Trajectory of center position.

In the above equations,  $M_{1f}$ ,  $M_{fp}$  and  $M_{p2}$  indicate the rotation conversion matrix for an angular speed of  $\phi_1$ , the translation conversion matrix for a translational speed of  $-e$ , and the rotation conversion matrix for an angular speed of  $\phi_2$ , respectively.

The absolute coordinate system is necessary for data analysis in the simulation program. Therefore, in the absolute coordinate system,  $\bar{r}_1$  and  $\bar{r}_2$  (obtained from the external tooth wheel  $r_1$  and the internal tooth wheel  $r_2$ , respectively) are calculated as follows.

$$\bar{r}_1 = M_{pf} M_{f1} r_1 = \begin{bmatrix} x_1 \cos \phi_1 - y_1 \sin \phi_1 + e \\ x_1 \sin \phi_1 + y_1 \cos \phi_1 \\ 0 \\ 1 \end{bmatrix} \quad (21)$$

$$\bar{r}_2 = M_{p2} r_2 = \begin{bmatrix} x_2 \cos \phi_2 - y_2 \sin \phi_2 \\ x_2 \sin \phi_2 + y_2 \cos \phi_2 \\ 0 \\ 1 \end{bmatrix} \quad (22)$$

The aforementioned trapezoidal tooth profile moves according to these equations of motion.

**2.4 Definition of the declination coefficient**

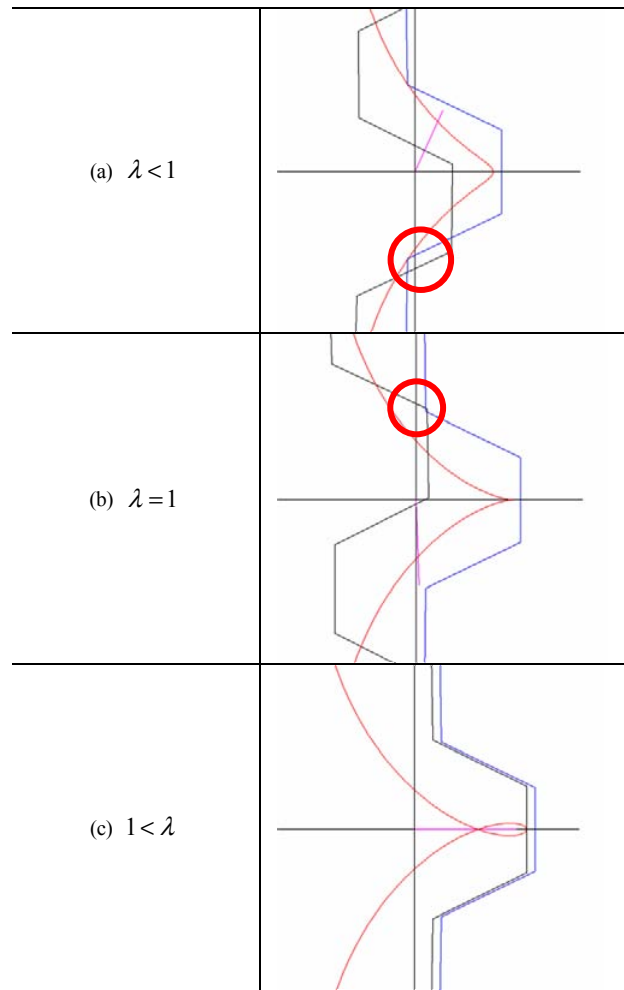
To determine the trajectory of the center of the external tooth wheel, the following equations for trajectory are used, with the tooth center set as  $(x_c, y_c)$  :

$$\begin{cases} x_c = H \times \cos(\theta \times R) + e \times \cos \theta \\ y_c = -H \times \sin(\theta \times R) + e \times \sin \theta \end{cases} \quad (23)$$

Here, the definitions are as follows:

$$H = \frac{mZ_f}{2} + 0.5m \quad (24)$$

Table 1. Change in tooth profile trajectory as a function of declination coefficient  $\lambda$ .



where

$$\theta = \frac{2\pi}{Z_f} \times i, \quad R = \frac{2}{Z_f}$$

Table 1 shows the results of evaluation of the trapezoidal tooth profile trajectory with respect to changes in the value of declination coefficient  $\lambda$ .

When  $\lambda=1$ , the end of the tooth surface encounters interference because of its position movement (as shown in red circle of Table 1(b)). This interference becomes greater because of the cycloid movement of the tooth when  $\lambda < 1$  (as shown in red circle of Table 1(a)). However, when  $1 < \lambda$ , there is no interference because tooth contact occurs in a direction opposite to that of tooth movement.

**3. Experimental results.**

**3.1 Prototype reducer for robot**

A prototype reducer for robots (shown in Fig. 7) based on our analysis results from the previous section is manufactured.



Fig. 7. Prototype of reducer for robots.

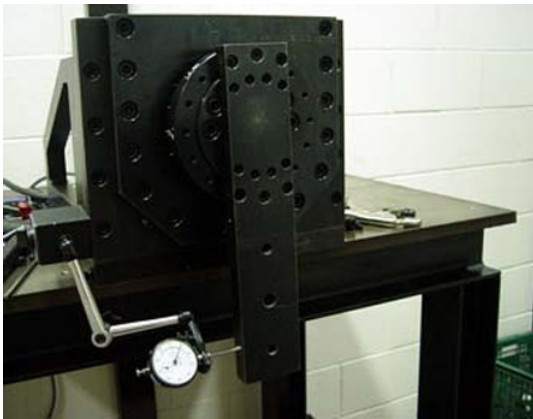


Fig. 8. Test bed for lost motion.

Then the data presented below from tests of this trial product is derived.

Sag stiffness amounted to 609 Nm/arc min and the sag load moment was measured as 1131 Nm. The maximum sag moment load was 2262 Nm, and the application point size ranged from 83.71 mm to -8.14 mm. The axial direction load was 3408 N and the radius direction load was 12180 N. The standard distance along the radius direction was measured as 50 mm. The rated output torque was 500 Nm, and the rated output frequency was 15 rpm. The maximum permissible average output torque was 700 Nm, the permissible speed increase/decrease torque was 1250 Nm, and the maximum permissible instantaneous torque was 2500 Nm. The maximum permissible output frequency was 27 rpm, the rotation precision was measured as lower than 1 min, and the torsion stiffness was 206 Nm/arc min.

### 3.2 Lost motion

To confirm the effectiveness of the developed tooth profile design, we manufactured a model with the following specifications. The manufactured model (HDXD050S-B148-S-S2) had a speed reduction ratio of 148:1, and lost motion was measured (using a test bed manufactured specifically to measure lost motion, as shown in Fig. 8) to be an average of 0.12

Table 2. Change in tooth profile trajectory as a function of declination.

	Displacement [mm]	Force [kgf]	Moment stiffness [Nm/arc min]
1	0.096	50	480.21
	0.048	30	576.25
	0.013	15	1063.9
2	0.098	50	470.41
	0.045	30	614.67
	0.011	15	1257.28
3	0.094	50	490.43
	0.05	30	553.2
	0.018	15	768.33
Average			697.18



Fig. 9. Test bed for bending moment.

arc min, thus satisfying the requirement for robots (less than 1 min).

### 3.3 Moment stiffness

When designing robots, a high value of moment stiffness must be used, because if the stiffness is not high enough, the resulting low eigenfrequency decreases the precision of the robots, and they sag under additional loads. The stiffness of currently available robots amounts to about 600 Nm/arc min.

In this study, based on experiments performed with the manufactured test bed (see Fig. 9) to measure the bending moment, the moment stiffness of robot reducers with a trapezoidal tooth profile was found to be greater than 600 Nm/arc min, which is a standard value of stiffness for robots (see Table 2).

Note: Distance to the forced point: 1000 mm; distance measured: 300 mm

### 3.4 Noise measurement

Table 3 lists the measured values of noise when a single reducer was operated under Nyquist control and noise was measured at a distance of 1 m from the source. Given that the average noise of industrial robot reducers is 85 dB, our prototype has a considerable advantage in terms of noise.

Table 3. Noise test.

Input speed [rpm]	Noise [dB]	
	Forward	Backward
1000	68	70
2000	73	74
3000	74	76

#### 4. Conclusion

The tooth profile of robots can be categorized as cycloid, involute, or trapezoidal. Our study evaluated the gearing features of the trapezoidal tooth profile. In addition, the applicability of the profile to robots was verified via prototype manufacture and laboratory experiments. Based on the results of our study, we proposed a new robot reducer tooth profile with a number of improvements with regard to gearing. In summary,

(1) Great improvements in gearing, stress, and stiffness by optimizing the declination coefficient have been introduced. A standard value of stiffness for general industrial robots is 600 Nm/arc min, but average value of stiffness for reducer using trapezoidal tooth profile is 697 Nm/arc min. It shows that newly designed trapezoidal tooth profile is structurally sound.

(2) Newly designed trapezoidal tooth profile make surface-contact, whereas the previous cycloid tooth profile make line-contact. Therefore the trapezoidal tooth profile has an advantage in terms of stress and bending stiffness by comparing its strength with that of the previous cycloid tooth profile.

(3) Reducer using trapezoidal tooth profile makes noise about 68–76dB in case input speed is from 1000 to 3000rpm. This shows proposed reducer offers improved noise reduction capability in comparison with previous reducer which makes noise about 85dB.

#### Acknowledgment

This research was supported by Chung-Ang University Research Scholarship Grants in 2010.

#### Nomenclature

$D$  : Diameter  
 $e$  : Eccentric coefficient  
 $m$  : Module  
 $M$  : Conversion matrix  
 $Z$  : Tooth number of gear  
 $\alpha$  : Pressure angle  
 $\lambda$  : Declination coefficient  
 $\phi$  : Angular speed

#### References

[1] D.W. Botsiber and L. Kingston, Design and performance of cycloid speed reducer, *Mach. Des.*, June (1956) 407-414.

- [2] J.G. Blanche and D. C. H. Yang, Cycloid drives with machining tolerances, *J. Mech. Transm. and Automat. Des.*, 111 (1989) 337-344.
- [3] T. Seiki, RV Series, *Catalog* (2001).
- [4] Harmonic Drive System, Harmonic Drive, *Catalog*, 4-12, (2000).
- [5] Y.-W. Hwang and C.-F. Hsieh, Geometric Design Using Hypotrochoid and Nonundercutting Conditions for an Internal Cycloidal Gear, *J. Mech. Des.*, April, 129 (4) (2007) 413-420.
- [6] F. L. Litvin, The synthesis of approximate meshing for spatial gears, *J. Mech.*, 3 (1968) 131-148.
- [7] Y. C. Tsai and P. C. Chin, Surface geometry of straight and spiral bevel gears, *ASME Trans., J. Mech. Transm. Automat. Des.*, 109 (1987) 443-449.
- [8] C. C. Lin and L. W. Tsai, The trajectory analysis of bevel gear Trains, *ASME Trans., J. Mech. Des.*, 115 (1993)164-170.
- [9] H. S. Yan and J. Y. Liu, Geometric design and machining of variable pitch lead screws with cylindrical meshing elements, *ASME Trans., J. Mech. Des.*, 115 (4) (1993) 490-495.
- [10] H. S. Yan and T. S. Lai, Geometry design of an elementary planetary gear train with cylindrical tooth-profiles, *Mech. Mach. Theory*, 37 (6) (2002) 757-767.
- [11] Sumitomo Machinery Corp. of America, SM-Servo-Match Precision Torque Multiplying Component, *Catalog* (2001).
- [12] SEJINiGB, Xcellent series, *Catalog*, 18-20 (2006/2007).
- [13] F. L. Litvin, Theory of Gearing, *NASA Reference Publication*, 1212 4-14.



**Se-Hoon Oh** received his Ph.D. Degree from Imperial College of U.K.. Dr. Oh is currently a Professor at the Department of Mechanical Engineering at Chung-Ang University in Seoul, Korea. His research interests include robotics, Harmonic driver system, Cycloid speed reducer and Bicycle



**Won-Ki Nam** received his B.S. degree in 2006 and M.S Degree in 2008 from Chung-Ang University of Korea, and is currently a Ph.D. candidate in Department of Mechanical Engineering at Chung-Ang University in Seoul, Korea. His research interests include robotics, Harmonic driver system, Cycloid speed reducer and designing of tooth profile.